Final Technical Report

Submitted to the
U.S. Geological Survey

by the Seismological Laboratory
California Institute of Technology

and by the Dept. of Geophysics
University of Utah

Grant No: G17AP00002 (Caltech)
G17AP00003 (Utah)

Principal Investigators:

Dr. Robert W. Clayton
Caltech
Seismological Laboratory, MC 250-21
Pasadena, CA 91125
clay@gps.caltech.edu

Dr. Fan-Chi Lin
Dept. of Geology and Geophysics
University of Utah, FASB 271
Salt Lake City, UT 84112
FanChi.Lin@utah.edu

Government Technical Officer

Jill Franks
External Research Support Manager
Earthquake Hazards Program, USGS

Title of Work:

Analysis of a New Broadband Survey Across the San Bernardino Basin to Determine Velocity and Structure: Collaborative Research Between the California Institute of Technology and the University of Utah

Program Objective: I & III
Effective Date of Contract: 12/01/2016
Expiration Date: 11/30/2017

Period Covered by Report: 12/01/2016 – 11/30/2017

Date: Feb 2, 2018

Analysis of a New Broadband Survey Across the San Bernardino Basin to Determine Velocity and Structure: Collaborative Research Between the California Institute of Technology and the University of Utah

U.S. Geological Survey Award No. G17AP00002

Key words: San Bernardino Basin, seismic structure, dense node array

Robert W. Clayton
Seismological Laboratory, California Institute of Technology
Pasadena, CA 91125

Fan-Chi Lin
Dept. of Geology and Geophysics, University of Utah
Salt Lake City, UT 84112

Abstract

We present preliminary results from node lines deployed across the San Gabriel and San Bernardino Basins in the greater Los Angeles. The overall goal of the surveys is to construct 3D models of these northern basins in order to confirm that they act as conduits to channel surface energy from the southern Andreas Fault into downtown Los Angeles. Three lines were acquired nearly simultaneously for approximately 30 days- two in the San Gabriel Basin and one in the San Bernardino Basin. The data and preliminary results show that dense node lines in a noisy urban environment is a fast and efficient manner for collecting data to study sub-surface structure. The ambient noise correlations show Rayleigh and Love waves that are used to determine the velocity via eikonal tomography. The noise autocorrelations derived from the noise correlations, and the receiver functions using teleseismic earthquakes show the basin bottom.

Introduction

This project was motivated by a study by Denolle et al (2014) that showed that the strong motions of earthquakes on the southern San Andreas Fault were under predicted in downtown Los Angeles by a factor of four. The "earthquakes" were generated from Green's function obtained from ambient noise correlation, and the predicted motions were from a numerical simulation using the SCEC velocity model. One explanation for the discrepancy is that the northern basins (San Gabriel and San Bernardino) were not adequately represented in the SCEC model and that they acted as "channels" focusing surface waves into the downtown area.

Figure 1. The 2017 Basin deployment lines. The SG1 and SG2 lines are in the San Gabriel Valley, while the SB4 line is in the San Bernardino Basin. The three lines were each deployed for approximately 5 weeks and the temporal overlap of the line was 3 weeks.

Northern Basin Surveys

Under this award, a dense node array was deployed across the San Bernardino Basin (line SB4) in order to determine the shear-wave velocity and the structure of the basin. A total of 92 three-component (3C) nodes were deployed along the line shown in Figure 1, for a period of 36 days. The node instruments were supplied by the University of Utah (Fan-Chi Lin). We obtained close to a 95% data recovery, with one station being stolen during the survey. The data were stored into hour-long segments for each station/component. The datasets were then distributed amongst the participating institutions. In addition to the SB4 line, we also recorded two lines in the San Gabriel Basin (SG1 and SG2) with 60 and 50 nodes respectively. The instruments were supplied by IRIS and Louisiana State University (LSU). All three lines had a temporal overlap of 3 weeks. This report shows examples of the data that were recorded and the analysis techniques being used to determine the velocity and structure of the northern basins in the Los Angeles region.

The deployment on each line was done by 5-6 crews that would permit and deploy all in the same operation. Most were deployed in private residences and in these cases the teams would knock on the door, ask permission, deploy the sensor in the front yard to facilitate pickup, note the location, and take a picture. To maximize the chances of finding people at home, the deployments were done on the weekend. Each crew was given a set of dots on a map, and asked to deploy within ½ block of the dot if possible. Some of the sites were in public parks, in which the nodes were well-hidden. The recording on all nodes was started at Caltech on the morning of the deployment, and was terminated when they returned to Caltech.

Ambient Noise Correlations

The data were correlated over the entire deployment time. Each station-component (s-c) was correlated with all other s-c's after they had been rotated into Z-R-T space (vertical-radial-tangential). The correlations were done by the procedure outlined in Lin et al (2013). The results are a set of virtual source gathers, examples of which are shown in Figure 2. These gathers show surface waves (Rayleigh and Love) and confirm that node type instruments can be used in a noisy urban environment. Successful correlations were obtained for periods from 1 to 5 sec.

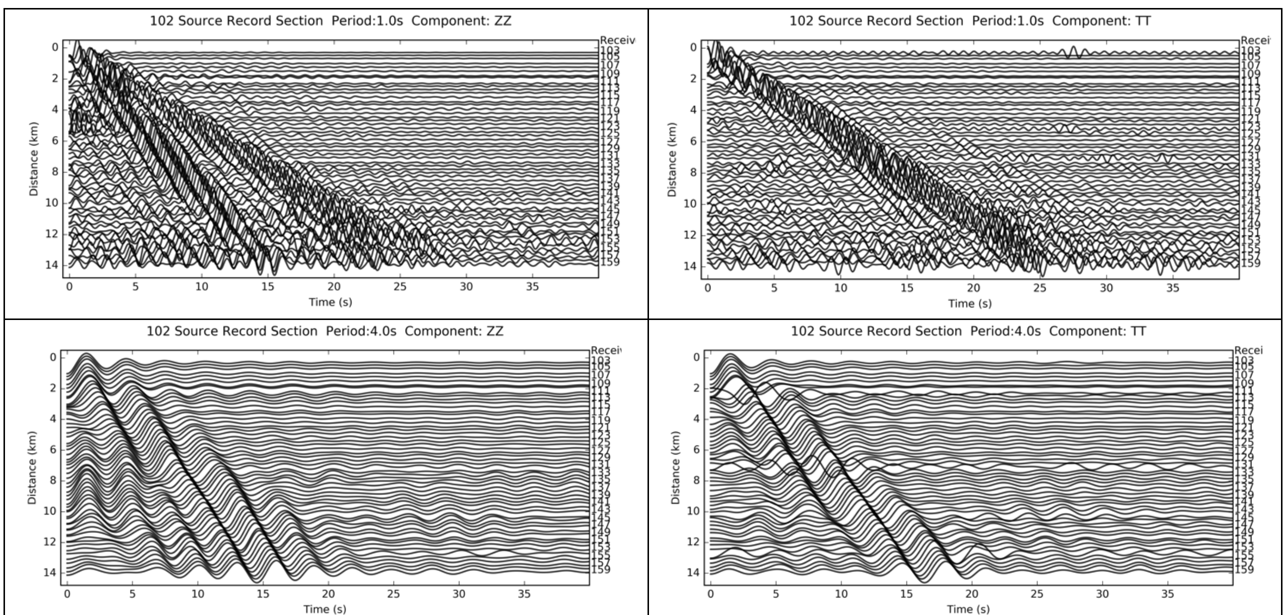

Figure 2. Examples of Symmetric Ambient Noise Correlation. The left panels shows the ZZ (vertical-vertical) correlations for SG1 where Rayleigh waves can be clearly observed. The right panels show the TT (tangential-tangential) correlation, and here the Love wave can be clearly seen. The top row is for correlations band-passed near 1 sec period, while the bottom is for 4-sec correlations. The fundamental mode is clear in all panels, while the upper-left also shows the 1st-overtone of Rayleigh waves. In all panels, the line is north-south, with north on the top.

Surface-Wave Velocity Determination

The phase velocities for the fundamental Rayleigh waves are determined from the ZZ correlations with an eikonal tomography approach (Lin et al, 2013), where the spatial gradient of the travel time is used to estimate the local slowness. The results for the SG1 line are shown in

Figure 3. They show that the slow phase velocities extend deeper than previous models. The phase velocity determinations were done by Elizabeth Berg and Fan-Chi Lin at Utah.

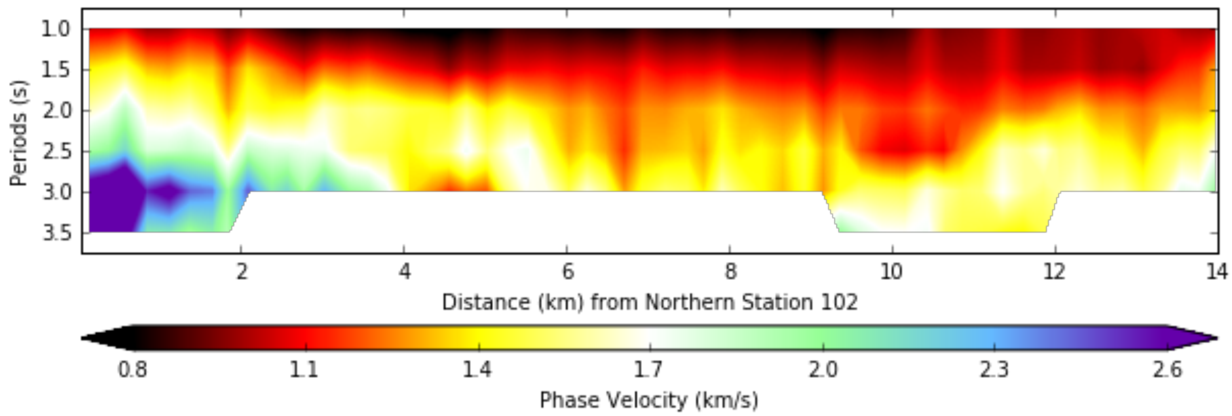

Figure 3. Phase velocity profile. The cross section shows the Rayleigh wave phase velocity along line SG1. North is on the left on the plot.

Autocorrelation Imaging

To form a structural image of the basin, a zero-offset section was created by stacking nearby offsets along the line. This effectively creates an autocorrelation section that can be used to image the subsurface reflectivity. The basic theory is given in Claerbout (1968). An example of this is shown in Figure 3. Here sections created from the ZZ correlations (P-wave image), TT correlations (SH-wave image), and the RR correlations (SV-wave image) are shown. They have been each time-to-depth converted using constant velocities of Vp=2.6 km/s and Vs=1.5 km/s.

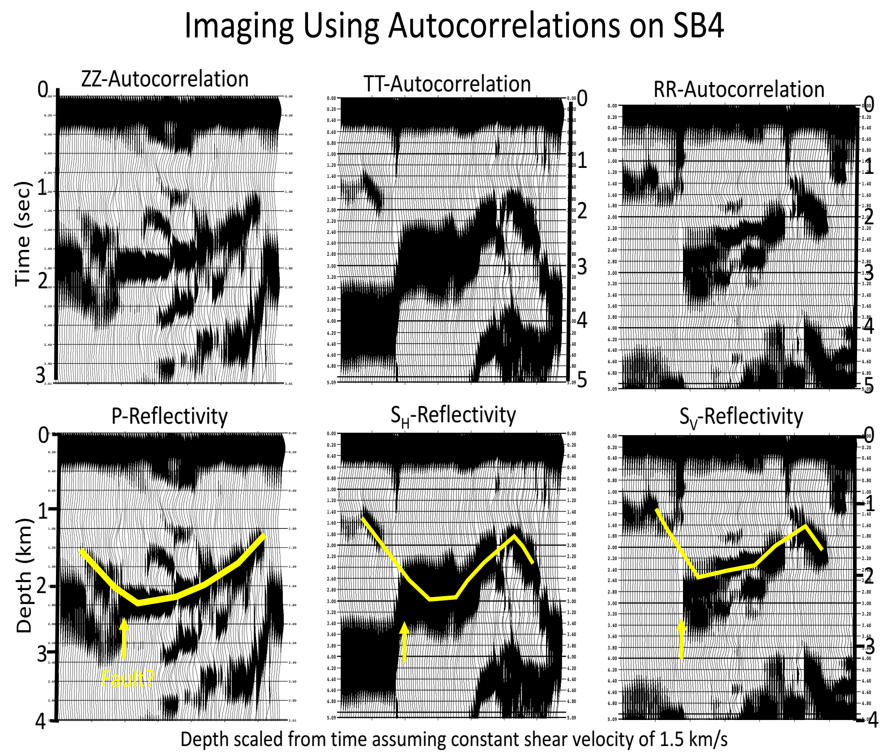

Figure 4. Autocorrelation Imaging Along SB4. The top row shows the autocorrelation images using the ZZ, TT and RR correlations. The horizontal distance is the full 29 km length of the SB4 line and north is on the left. The bottom row is a simple time to depth conversion applied with Vp=2.6 km/s and Vs=1.5 km/s. The yellow lines are an interpretation of the basin bottom, which is similar but exactly the same in the three sections. There is also an indication of a fault in the basement about 8k from the north end of the line.

Teleseismic Earthquake Recordings

During the course of the deployment two teleseismic earthquakes were recorded. There are:

Bolivia, 2017/02/21, M6.5, lat=-19.281, lon=-63.905, depth=596km

Fiji area, 2017/02/24, M6.9, lat=-23.260, lon=-178.803, depth=396km

These events are shown in Figure 5, and although they are smaller than earthquakes commonly used in receiver functions, they have a larger high-frequency level because of their large depth. The high-frequency content is important for imaging shallow structure.

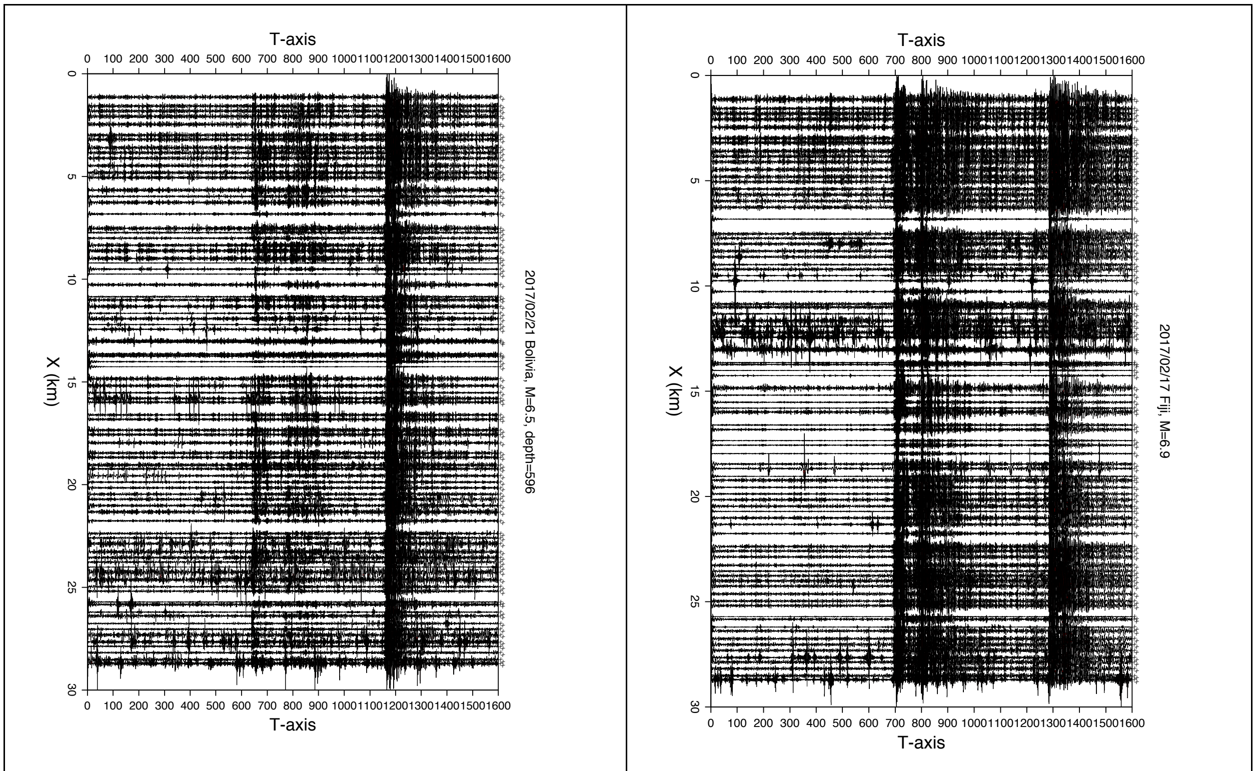

Figure 5. Recordings of Teleseismic Events. During the deployment, deep earthquakes from Fiji and Bolivia provided events for receiver function imaging of the basins. In both panels, the first arriving energy is the P-wave, and the last is the S-wave.

Receiver Functions

Receiver functions for the teleseismic events were created using the standard method for Ps imaging. The results are shown in Figure 6, and were done by Guibao Liu and Patricia Persaud of Louisiana State University using a procedure similar that decribed in Ma and Clayton (2016). The image appears to show the basin bottom, and a mid-crustal layer, and the Moho. In addition, there may be a fault that is indicated in Figure 6. This fault, if it is real, is between the mapped San Jose Fault and the Red Hill Fault (Cramer and Harringtion, 1987).

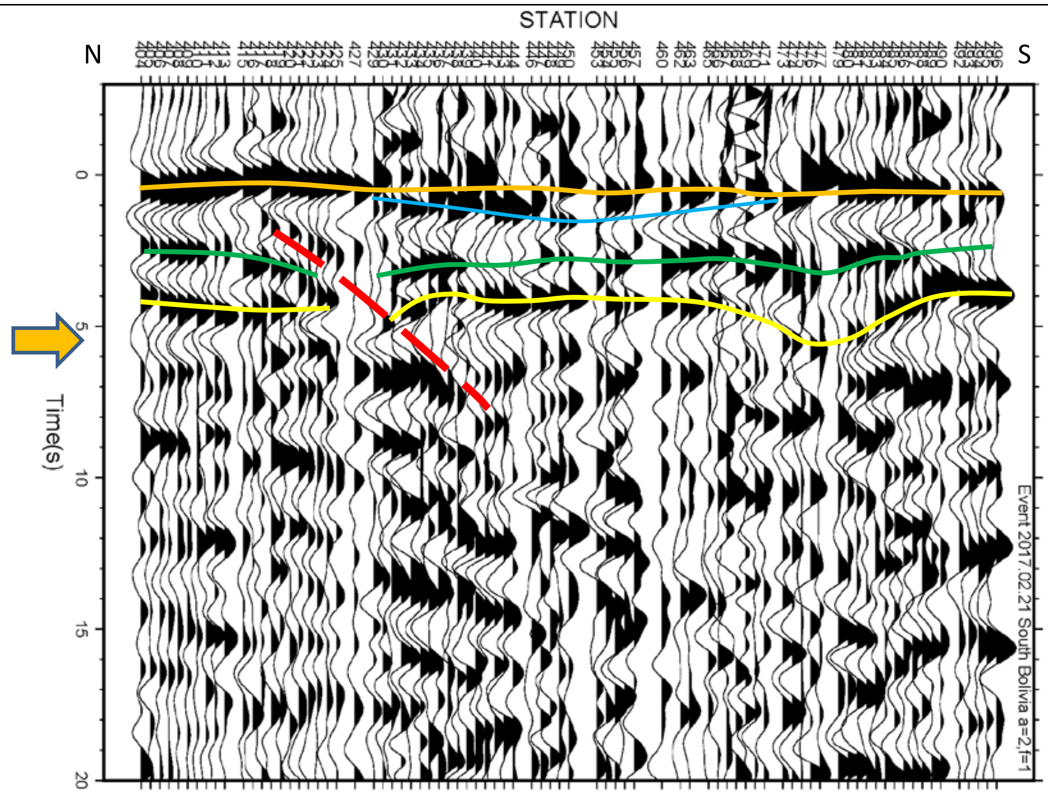

Figure 6. Receiver function image formed from the P-wave arrival of the earthquakes shown in Figure 5. The blue is the deposition center of the basin. The orange is the basin bottom, the green is a mid-crust arrival and the yellow is the Moho. We also interpret a possible fault shown by the red line. This is coincident with the fault location shown in Figure 4. The receiver function image shown here was created by Guibao Liu and Patricia Persaud of LSU.

Discussion and Conclusions

The results of this survey are at a preliminary stage. However, they do show that the technique of dense passive arrays in a noisy urban environment. They also appear to show that the basins are deeper and slower than predicted by the various SCEC models. This lends credence to the idea that the northern basins are a conduit that funnels strong surface wave energy from the southern San Andreas Fault to downtown Los Angeles.

We are planning an additional 3 lines in the San Bernardino basin area. We believe these will be done in 2018. We will use the data from all six lines to cross-correlate with the 10 SCSN stations in the area to form a 3D model of the basins.

References

Cramer, C. and J. Harrington, (1987), Seismicity and Tectonics of the Cucamonga Fault and Eastern San Gabriel Mountains, San Bernardino County, in Recent Reverse Faulting in the Transverse Ranges, California, US Geol. Surv. Professional Paper 1339, 7-26.

Claerbout, J., (1968), Synthesis of a layered medium from its acoustic transmission response, Geophysics, 33, 2 264-269.

Denolle, M., E. Dunham, G. Prieto, and G. Beroza, (2014), Strong Ground Motion Prediction Using Virtual Earthquake, Science, 343, 399, doi:10.1126/science.1245678

Lin, Fan-Chi, D. Li, R. Clayton, D. Hollis, 2013, High-resolution shallow crustal structure in Long Beach, California: application of ambient noise tomography on a dense seismic array, Geophysics, 78(4), Q45-Q56, doi:10.1190/geo2012-0453.1

Ma, Y., R. Clayton (2016a), "Structure of the Los Angeles Basin from ambient noise and receiver functions", Geophys. J. Int. (September, 2016) 206 (3): 1645-1651.doi: 10.1093/gji/ggw236

Olsen, K. B., Day S. M., Minster J. B., Cui Y., Chourasia A., Faerman M., Moore R., Maechling P., Jordan T (2006) "Strong shaking in Los Angeles expected from a southern San Andreas earthquake", Geophysical Research Letters, Vol. 33, L07305, doi:10.1029/2005JL025472